SHEFEX II Precession Control

Josef Ettl[1] and John Turner[2]
DLR, RB-MR, Oberpfaffenhofen, Germany

The SHEFEX II sounding rocket vehicle comprised a two stage VS40 motor combination, whereby the first stage was passively aerodynamically stabilized by canted fins but the spinning second stage motor and payload, was repointed before ignition and controlled during its burn phase by a two axis, cold gas, precession attitude control system. The result was a suppressed trajectory with greatly reduced dispersion, which provided a significant increase in the time available for the re-entry thermal protection and canard guidance experiments and improved the possibility for down range tracking and data retrieval as well as sea recovery of the payload.

I. Introduction

THE purpose of the DLR experiment program SHEFEX, is to investigate the aerodynamic behaviour and thermal protection characteristics of new materials and unconventional shapes for re-entry vehicles comprising multi-facetted surfaces with sharp edges. The main object of these experiments is the correlation of numerical analysis with real flight data, in terms of the aerodynamic effects and structural concept of the thermal protection system. SHEFEX I, launched on the 27th October 2005, comprised an asymmetrical forebody and passive reentry at Mach 6-7. The SHEFEX II experiments comprised a symmetrical forebody, a hybrid navigation system and active canard control during reentry at a velocity in the region of Mach 10. The Mobile Rocket Base MORABA, of the German Aerospace Centre (DLR), was responsible for the development and qualification of the vehicle and service systems for the test flight of SHEFEX II on a two-stage solid propellant VS 40 sounding rocket vehicle system. After separation from the first stage motor and prior to ignition, the second stage motor and payload were actively re-pointed while spinning, by a cold gas precession attitude control system. The purpose of this manoeuvre was to provide a suppressed trajectory with a greater horizontal velocity and range and a flatter reentry trajectory. This resulted in a longer experiment period during the atmospheric re-entry between the altitudes of 100 and 20 kilometres, at a velocity in the order of Mach 10. A further significant advantage was the considerable reduction in impact dispersion to increase the possibility of telemetry reception to a lower altitude by a downrange station on Spitzbergen and reduce the time for search and recovery of the payload by a ship. SHEFEX II was launched on June 22nd 2012 at 19:18 UTC from the Andoya Rocket Range in Andenes, Norway. This paper describes first the different cold gas control systems and the navigation system on board consisting of an IMU (rate gyroscopes and accelerometer) and a GPS system. Furthermore, the results of the control sequences are shown and evaluated.

II. Vehicle, System and Mission Developments

The trajectory calculated for the vehicle resulted in a ground range of 800 Km. As experiment data reception was required down to 20 Km altitude, the impact point was planned to be within 300 Km of the polar satelite tracking station at Longyearbyen on Spitzbergen. As there is a heavy shipping traffic between the Norwegian coastline and the islands of Svalbard, especially during the midsummer period when SKEFEX II was eventually launched, the three sigma impact dispersion of the first and second second stage motors and payload, posed a significant safety problem and resulted in an exceptionally large impact warning area. To satisfy the requirements of trajectory control and reduction of impact dispersion, attitude control for star camera reference updates, payload alignment with the instantaneous re-entry flight vector and angular rate damping during the atmospheric re-entry, four different cold gas control systems were designed to provide angular rate or attitude control for the vehicle and payload and comprised the following.

[1] Head of Electrical Flight Systems Group, DLR RB-MR, Germany, josef.ettl@dlr.de
[2] SHEFEX Project Engineer, contracted by DLR RB-MR, Germany, john.turner@dlr.de

- Roll spin rate control
- Two axis precession control
- Three axis attitude control
- Three axis rate damping

The first stage S 40 rocket motor was passively stabilized with canted fins to provide roll spin stabilisation in order to reduce the dispersion of its trajectory. In case the resulting roll rate at S 40 motor burnout differed significantly from the nominal spin rate of 1.5 Hz, required by the precession control for the second stage repointing, a roll spin rate control system was included in the motor payload adapter. This system comprised two solenoid valves in the aft end of the payload which each connected to dual thruster nozzles on the motor to payload adapter, for maximum moment arm. The thrust provided was two times 30 newtons for each thruster pair about the roll axis.

An online trajectory analysis program was developed which used navigation data from the inertial platform to predict the pointing vector required by the precession controlled spinning second stage S 44 motor and payload, to compensate for any error incurred during the first stage trajectory and achieve the optimum impact point for the data reception by the down range telemetry station and retrieval of the payload by the recovery ship. Assuming a nominal trajectory flight of the first stage motor, the required flight vector for the second stage burn was loaded into the control system shortly before launch. During the first one hundred seconds of flight, the actual trajectory data from the payload inertial platform comprising instantaneous position and velocity vector data was processed by the analysis program such that even in the event of drift of the actual trajectory during the passive stabilized first stage motor burn, a corrected pointing vector could be transmitted to the precession control system inflight to compensate the drift and still achieve the required flight path. The roll spin rate control system was not used in flight, as the desired spin rate of 1.5 Hz was achieved to within 0.1 Hz by means of the first stage motor fins. The two axis precession control was therefore activated earlier than planned and resulted in accurate repointing, including compensation by telecommand for the acquired trajectory drift during the passively stabilized first stage motor burn, well before the earliest second stage ignition target of T+150 seconds.

After burn out of the second stage, the spin rate was reduced to close to zero by a yo-yo system. The fairings and second stage motor were then ejected from the payload and a three axes attitude control system was activated to point an on-board star camera away from the sun. The task of the star camera was to calculate a precise attitude on the basis of known star positions and provide an inertial update to the experiment IMU. To avoid an interference with the sun, the star camera was moved into the shadow of the payload. After completion of the star update, the payload was realigned to the re-entry vector and then at the commencement of the experiment re-entry at 100 Km altitude, this control system was switched to rate control mode to provide rate damping during the experiment phase in order to reduce any aerodynamic induced oscillation of the payload about the flight vector. This function was switched off at an altitude of about 50 km on the descent phase, when the payload had achieved a velocity of the order of Mach 10. Below this altitude, the canard system took over the control of the payload attitude and rates. The actual impact was very close to the nominal impact despite a significant divergence of the first stage trajectory from nominal. At a range of more than 800 km the distance between the nominal and actual impact was only 8 km.

III. Inertial Sensors

A digital miniature attitude reference system,(DMARS) inertial platform, which was part of the autonomous service module, measured the attitude,velocity and acceleration, derived the instantaneous position and provided the rate and attitude control signals for the cold gas thrusters. As the experiment performance analysis was dependent on the accuracy of measurement of the angle of attack to the flight vector, GPS data was also used to provide independent accurate real time trajectory data, during the experiment phase and in the post flight analysis of the trajectory and attitude data.

Figure 1: DMARS Components

IV. Standard Cold Gas System

The following figure shows a typical cold gas control system. The number of working pressure levels, valves and nozzles depends on the requirements of the system. Whereas only three valves and nozzles and only one working pressure level were required for the precession system, two valves and four nozzles were necessary for the roll spin rate control and eight valves, eight nozzles and two levels of working pressure were incorporated for the three axes attitude and rate control system.

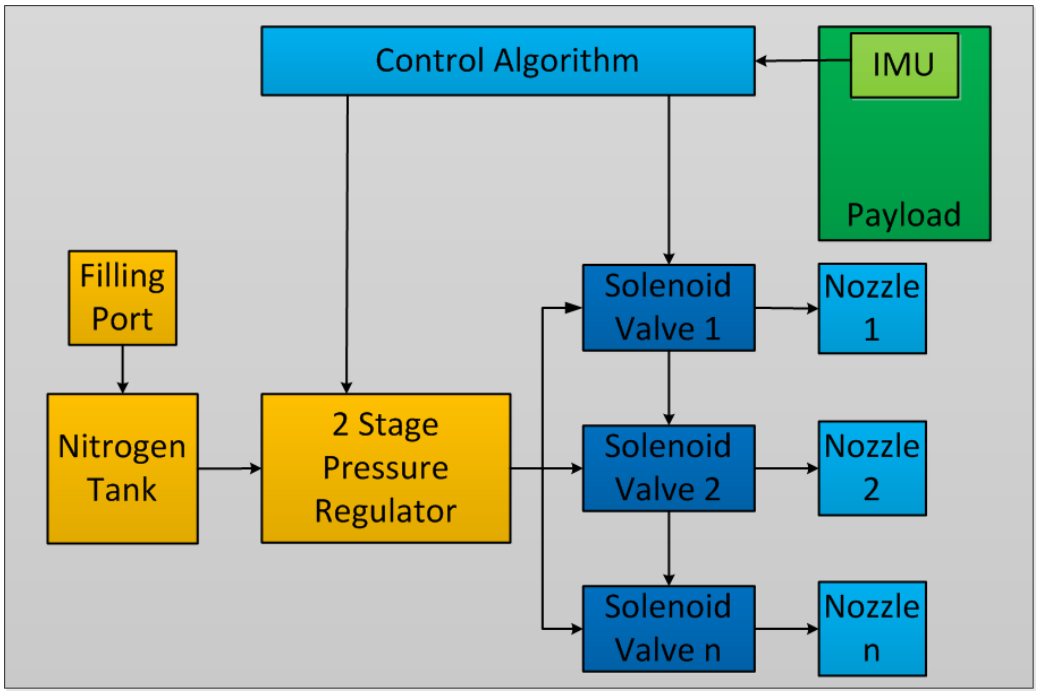

Figure 2: Principle Cold Gas System

V. Precession Strategy Principles

Precession manoeuvres may be performed in two principle ways. The most common method, as usually described in the literature, proposes a motion over a half cycle of the space cone, whereby the control impulse has always to occur perpendicularly to the desired motion. An alternative method of performing a precession manoeuvre is to move the longitudinal axis over very small segments of the space cone and to move the space cone towards the target. This method was more promising than the common procedure as a larger angular rate and faster control manoeuvre, could be achieved.

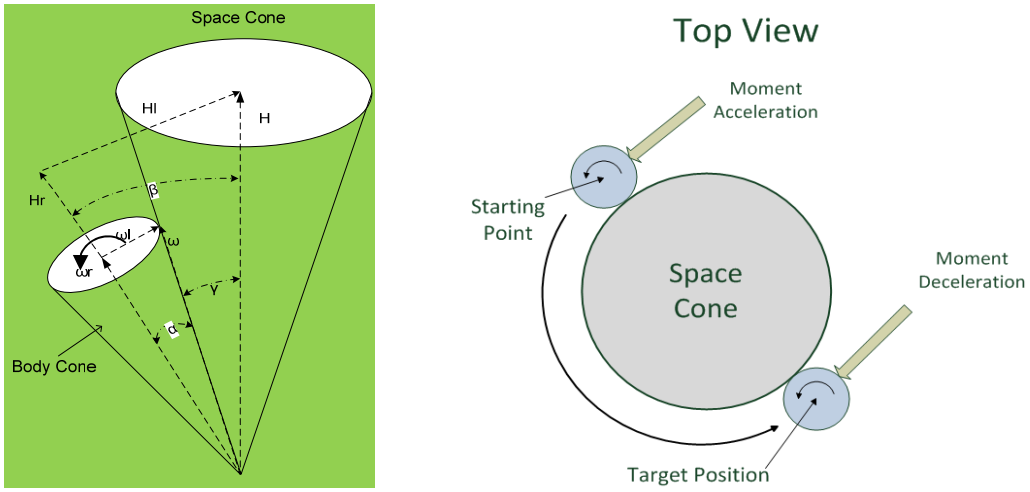

Figure 3: Precession Manoeuvre, moving over half space cone circle

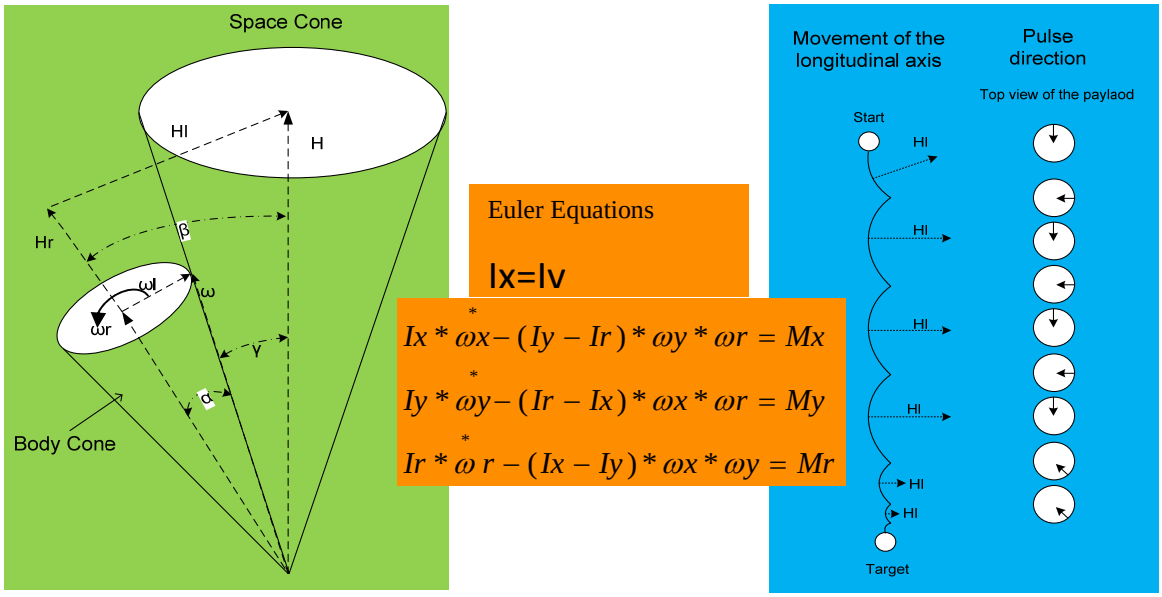

Figure 4: Precession Manoeuvre, moving over segments of the space cone

The figures above demonstrate the motion of the longitudinal axis towards the target. To perform this motion, only 3 different types of impulse are used.

a) Acceleration towards the target position
b) Correction pulse to keep the movement in one plane, perpendicular to the target direction
c) Braking pulse to reduce the angular rate and stop at the target position, against the moving direction

When the movement to the target position is accelerated, the sizes of the body and space cone increase. The limitation of the space cone depends on the moment which can be introduced per cycle and the moments of inertia of the roll and not of the lateral axes.
In our actual case, a maximum angular velocity of more than 3 degrees per second could have been achieved, but to keep the control system stable with a safe margin, a maximum angular rate of 2 degrees per second was chosen. Exeeding the limitations, which are shown for a system with one or three nozzles at the circumference, would mean that the motion performed in a plane would change over to a motion over the space cone, and the control system becomes instable. The limitation also strongly depends on the spin frequency.

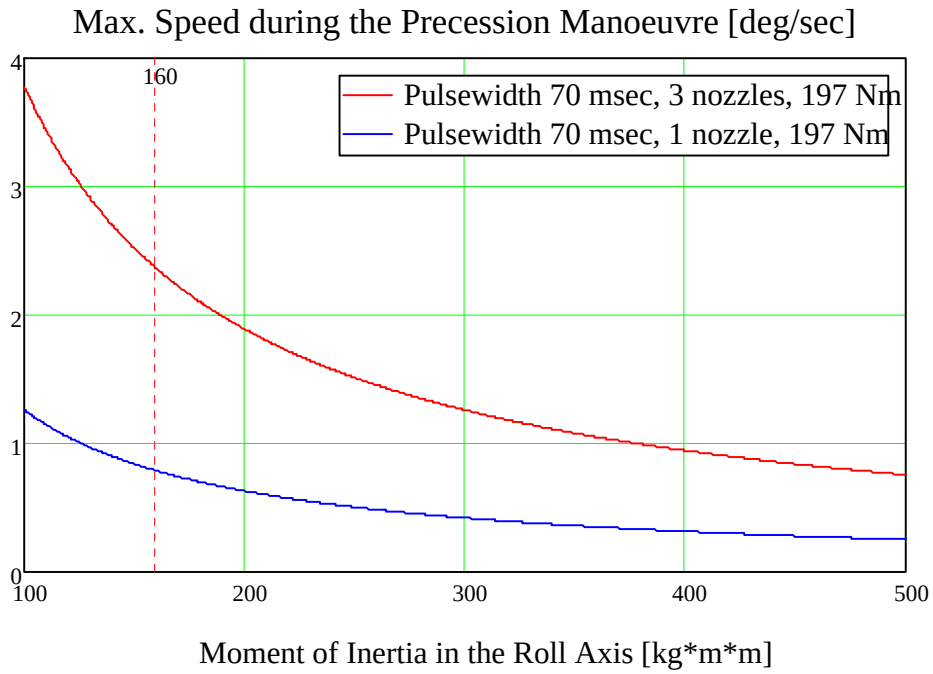

Figure 5: Different maximum slew rates (depending on 1 or 3 nozzle design) versus Roll moment of inertia

Generally, the higher the spin rate, the lower is the possible angular rate which can be achieved. This phenomenon is shown in the following graph. To make a compromise between the desired angular manoeuvre rate and the necessary spin rate for the reduction of the impact dispersion, 1.5 Hz was chosen.

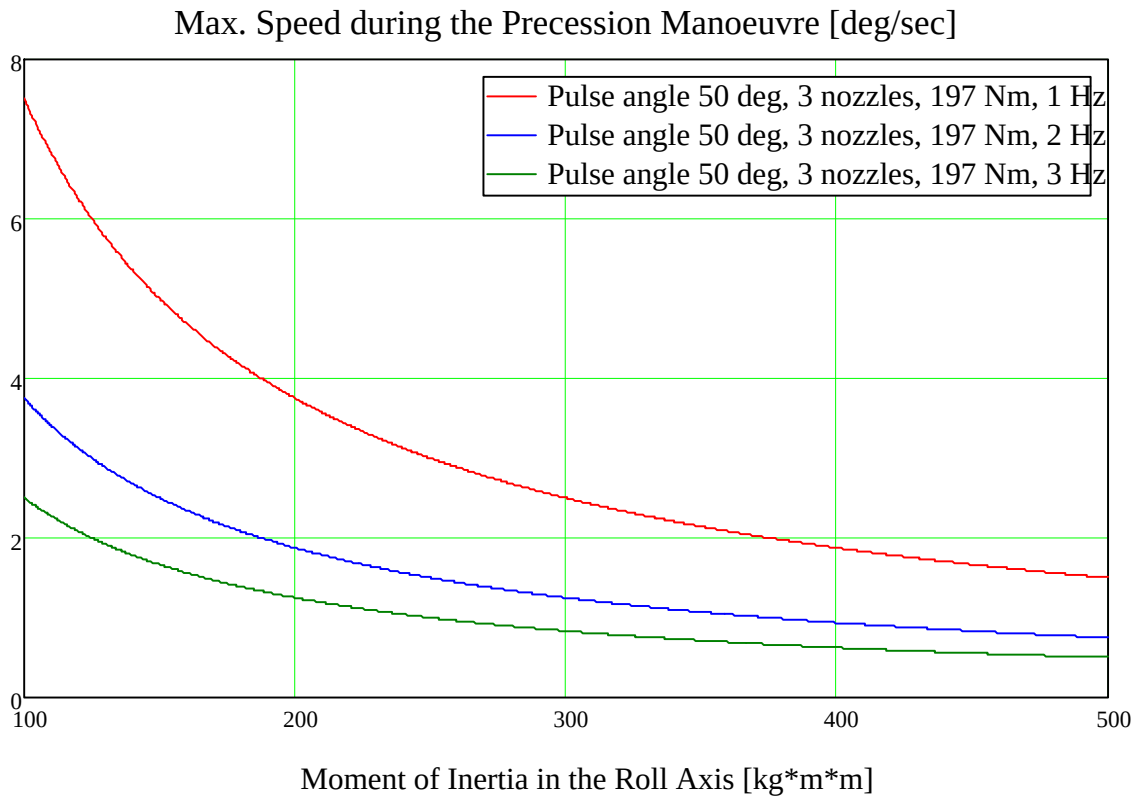

Figure 6: Different maximum slew rate (depending on the spin frequency) versus Roll moment of inertia

The precession control system moved the longitudinal axis of the spinning rocket to the desired attitude. The first attitude based on a nominal trajectory while the second commanded attitude was calculated online, including the actual position of the vehicle and the actual speed vector. Three 100N thrusters were used as actuators and produced a maximum angular slew rate of the order of 2 degrees per second. The DMARS platform delivered the necessary Pitch, Yaw and Roll angles and rates for the control systems and the control pulses.

VI. Simulation of a Precession Manoeuvre

The following graph shows the simulation of a precession manoeuvre. The superposed variety upon the pitch and yaw angles can be simulated by dynamic imbalances and by misalignments between the longitudinal payload axis and the roll axis of the IMU. The frequency of the oscillation above the Euler angles is the spin frequency as the longitudinal axis of the payload pivots in a plane. If the longitudinal axis would pivots over the space cone the oscillation above the Euler angles would be equal to the nutation frequency, which is a little bit less than the spin frequency as shown in the following nutation frequency equation.

$$freq\_nut = \frac{(I_{Roll} - I_{lat})* freq\_spin}{I_{Lat}}$$

$I_{\_Roll}$ = Moment of inertia about the Roll axis

$I_{\_lat}$ = Moment of inertia about the lateral axis

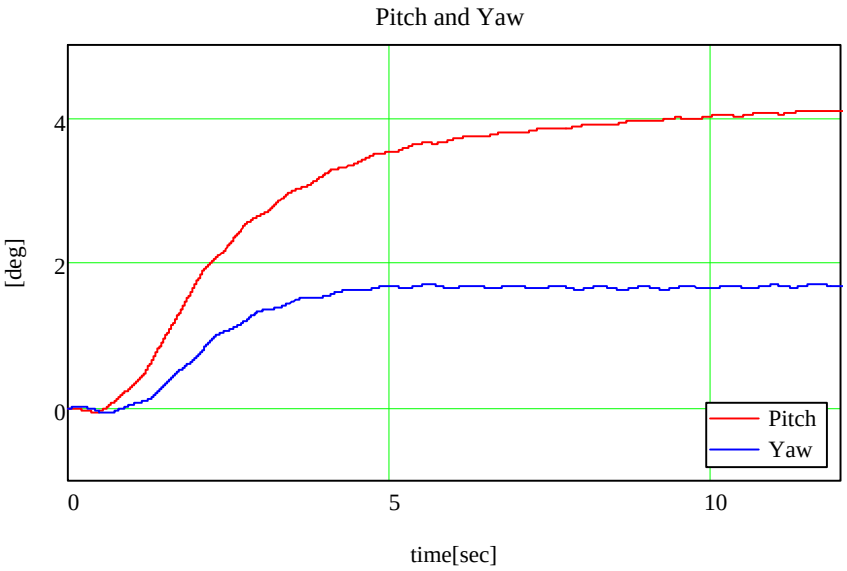

Figure 7: Simulated Pitch and Yaw angles during a Precession Manoeuvre

By the limitation of the space cone size (4 degrees half angle) the maximum slew rate of 2.5 deg/s is determined, which is fairly off the maximum angular rate, and therefore guarantees a stable movement. As the superposed oscillation causes a degradation of the control loop, it is advisable to eliminate this oscillation by the implementation of a notch filter.

VII. Notch Filter

The notch filter is an appropriate means to damp the spin frequency in order to improve the control attributes. As mentioned above, the oscillation with spin frequency is caused by imbalances and misalignments of the longitudinal axes. It is easy to design a variable notch filter in the control loop as the spin frequency is well known. As the spin frequency doesn't experience many variations, the bandwidth of the notch filter can be very small. This reduces its influence upon the control signal. A well dimensioned notch filter doesn't produce a phase shift or damping of the control signals.
The following figure shows the structure of a digital notch filter. By choosing the appropriate values d0-d2 and c0,c1 its notch frequency, bandwidth and its quality can be selected.

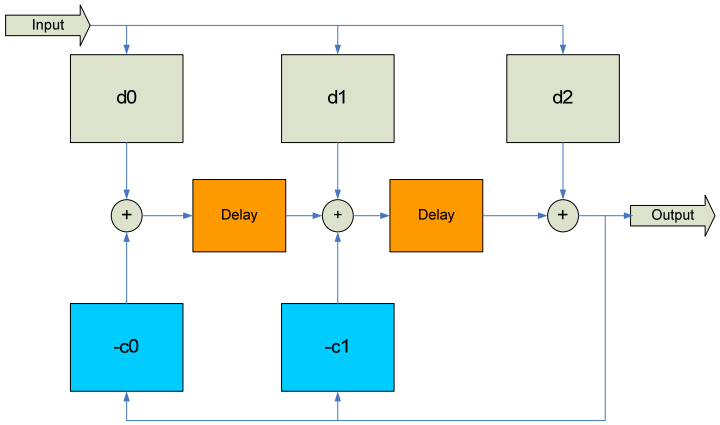

Figure 8: Notch Filter data flow diagram

The delay boxes are memories which store the value until the next sample occurs.

The simulation below indicates a good damping of the spin frequency which is superimposed upon the control signal. It is evident that the disturbing spin frequency is subtracted from the control signal.

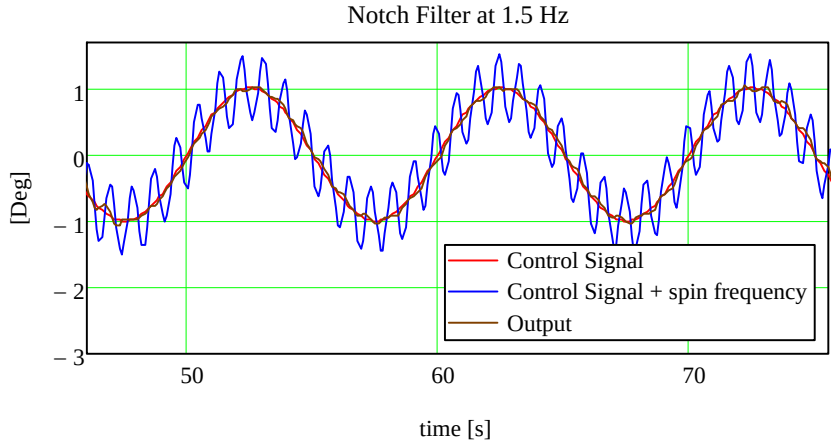

Figure 9: Control Signal overlayed by a nutation signal of about 1.5 Hz

VIII. Flight Performance during SHEFEX II Mission

The following figure illustrates the position of the precession control module.

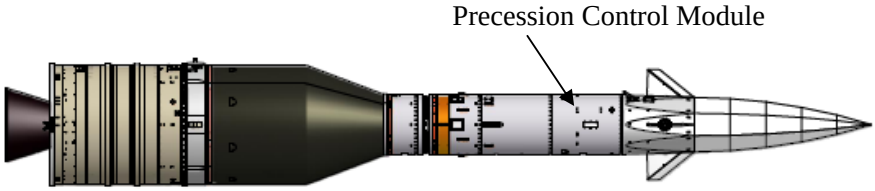

Figure 10: Second stage motor and payload configuration

Physical properties	Value
Roll, moment of inertia	160 kgm^2
Lateral, moment of inertia	3500 kgm^2
Roll, thrusters' moment arm	0.5 m
Lateral, thrusters' moment arm	3.5 m
Roll, thrust	2 * 100 N
Lateral, thrust	100 N
Roll, spin rate	1.5 Hz
Minimum pulse width	10 msec
Maximum pulse width	~70 msec
Number of nozzles	3

Figure 11: Physical properties

The following graphs illustrate the Pitch and Yaw Euler angles during precession manoeuvres between T+60.9s and T+184.6s. The first precession manoeuvre started at T+60.9 s and was finished at T+100 s. The correction by telecommand can be seen at T+120 s. The first precession manoeuvre was based on the pre-flight calculated, and stored values assuming zero deviation from the nominal trajectory during the first stage motor burn and was complete by T+100 seconds. During this period, realtime trajectory data was processed in a ground based computer and the corrected Euler angles were then sent to the vehicle, resulting in the re-acquisition occurred between T+120s and 184.6s, and also controlled the longitudinal axes while the second stage was burning.

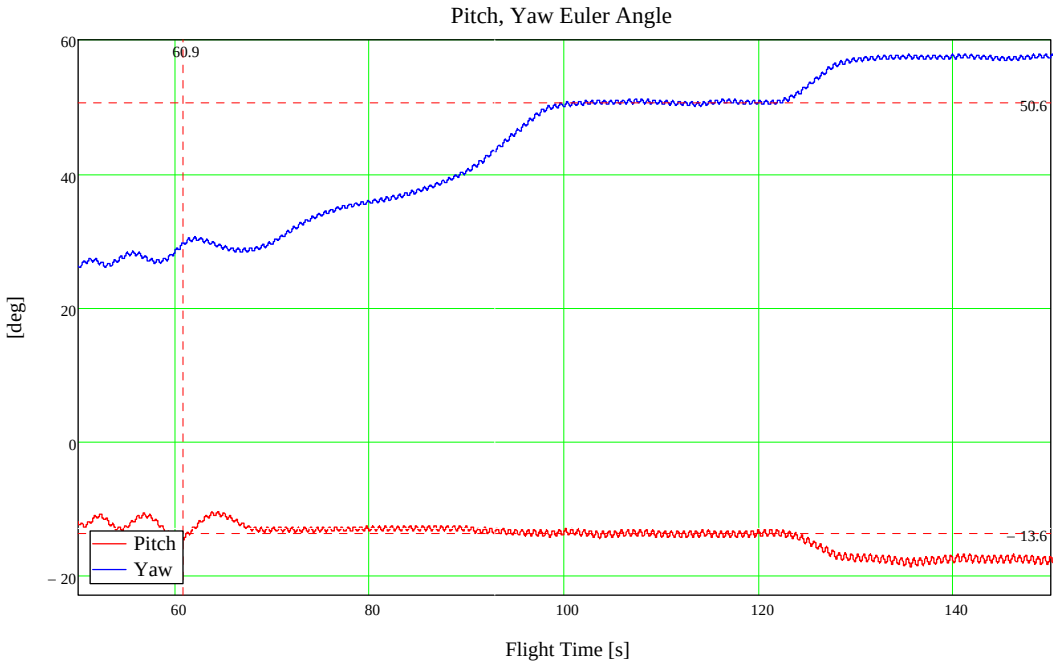

Figure 12: First and second Precession Manoeuvre

The precession control was left on during the beginning of the burn phase of the second stage. At T+184s the control was switched off. It is obvious that the precession control brought back the longitudinal axis into the desired position several times during the burn phase (see next graph). After the end of the precession control a slight drift is visible. At T+224s the YoYo system was activated, and the vehicle despun to a residual roll rate of about 10 deg/s.

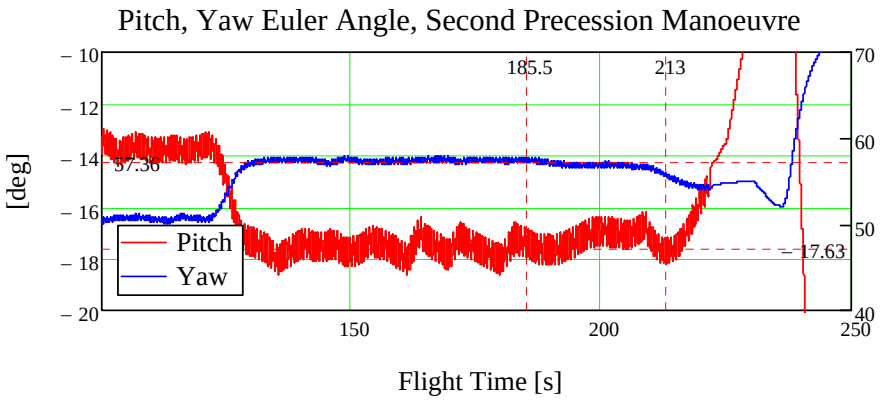

Figure 13: Precession Manoeuvre during second stage burn phase

During the spinning phase, a nutation of about ± 0.38 deg occurred. This nutation can be explained by inherent imbalances and axes misalignments between the longitudinal axis of the DMARS and the vehicle.

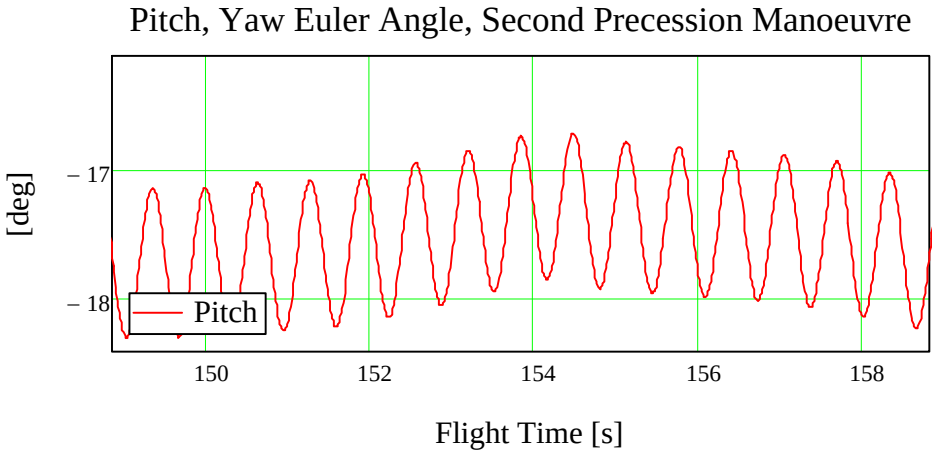

Figure 14: Nutation signal superimposed on the control signals

IX. FLIGHT DYNAMICS

The rocket reached an apogee of 178 km and a down range of 802 km. The maximum velocity achieved was more than 2.8 km/sec. The experiment phase was about 60 sec. During this time, highly valuable data could be received which will help us to understand the aero- and thermodynamic attitudes in supersonic ranges. Furthermore the thermal protection system (flat tiles) could be tested and verified.

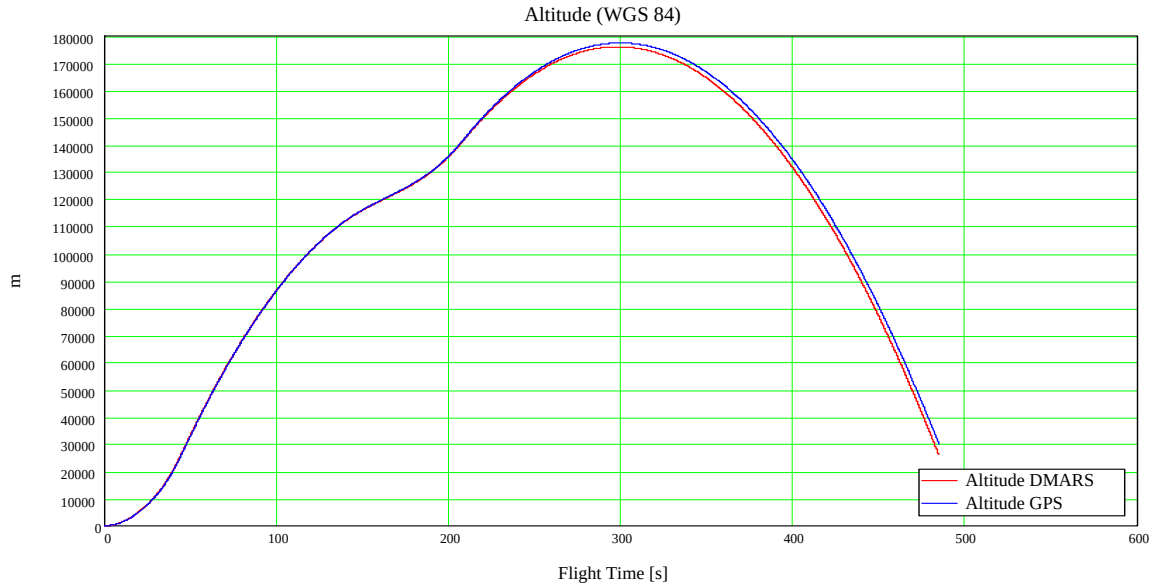

Figure 15: Altitude from DMARS and GPS

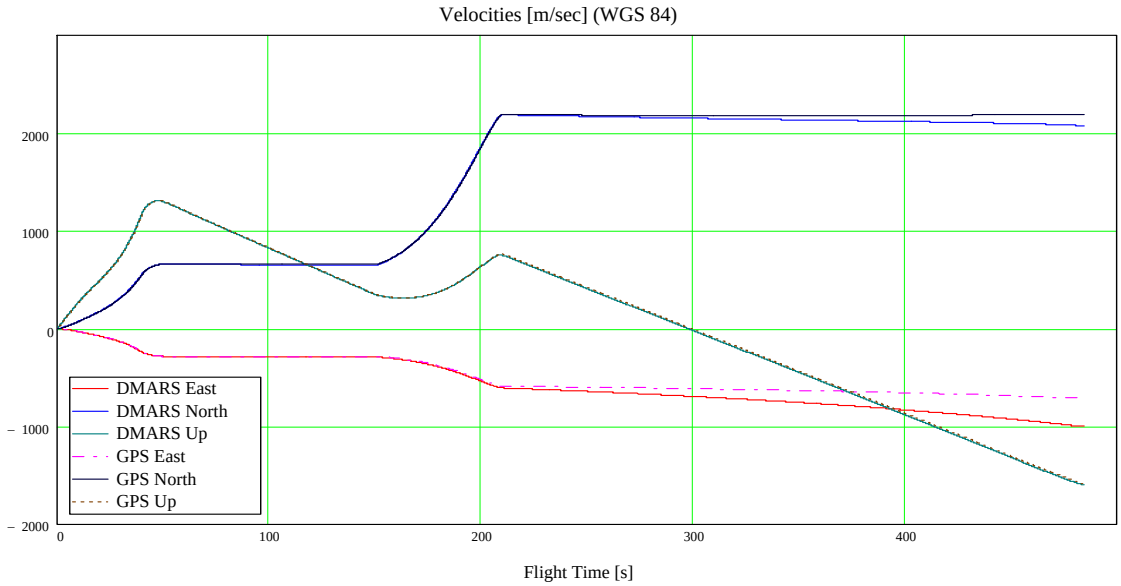

Figure 16: Velocity components in East, North and Up from DMARS and GPS

X. CONCLUSION

All the control loops performed well and displayed a high stability and accuracy. The navigation system, consisting of the DMARS and the DLR GPS system delivered highly reliable data during the flight. All cold gas control systems have been flight proven and can be used for further projects, such as SHEFEX III. By the means of the precession manoeuvre DLR Moraba actively controlled for the first time the trajectory of a sounding rocket.

XI. Acknowledgments

The authors thank the DLR program management, colleagues of MORABA, the members of the various experimenter groups and particulary the project manager Hendrik Weihs for their support for the successful flight of SHEFEX II.

XII. References

SHEFEX II System Specifications, by John Turner, 16th March 2010

Precession Manoeuvre, by Josef Ettl, 3rd March 2009

SHEFEX II Post-Flight Report, Flight Safety, by Frank Scheuerpflug, 6th July 2012

XIII. Figure List